 CMES, vol.91, no.1, pp.1-15, 2013

A transport model based on kinetic theory for water vapor separation in hollow fiber membranes

D. Bergmair[1,2], S. J. Metz[1], H. C. de Lange[2] and A. A. van Steenhoven[2]

Abstract: A method to predict the permeation of water vapor, present in a laminar flowing humid carrier gas, through a hollow fiber membrane is presented. The method uses simulation particles that move like molecules, according to the kinetic gas theory, but carry the physical properties of an ensemble of molecules which they statistically represent. With this approach an ideal operational window for membrane modules can be found and parameters tested for, can be varied over orders of magnitude. The results show that the right dimensioning is essential for the efficient use of the membrane area.

Keywords: modeling, simulation, statistical particle displacement model, hollow fiber membrane, dehumidification, gas separation

1 Introduction

Over the last decades, membrane technology has emerged as a major player in separation and purification technology . The main fields of applications nowadays are i.e. sea water desalination [Fritzmann, Löwenberg, Wintgens, and Melin (2007)], fresh water purification [Shannon, Bohn, Elimelech, Georgiadis, Mariñas, and Mayes (2008)], gas separation/purification [Baker (2002)], as well as offering alternatives to distillation processes [Smitha, Suhanya, Sridhar, and Ramakrishna (2004)] . However there are many more areas of application where membrane process hold the potential for improving performances like e.g. the water vapor extraction from ambient air to produce fresh water. In such an application the separation of the water vapor from the rest of the air could reduce the energy requirement for cooling/condensation by more than 50% [Bergmair, Metz, de Lange, and van Steenhoven (2012)].

In order to minimize costs for such a process, and to find the ideal working conditions, the modeling of a membrane module has become a valuable tool. Numerous

[1] Wetsus-Centre of Excellence for Sustainable Water Technology, Agora 1, Leeuwarden, NL
[2] Technische Universiteit Eindhoven, Den Dolech 2, Eindhoven, NL

methods and models have been developed to suit any geometry and working conditions [Marriott and Sørensen (2003)]. In the case of hollow fiber modules, a variety of models exist using either self made finite volumes element methods [Cruz, Santos, Magalhaes, and Mendes (2005)], commercial Computational Fluid Dynamics (CFD) software [Ghidossi, Veyret, and Moulin (2006); Marriott, Sørensen, and Bogle (2001); Scholz, Harlacher, Melin, and Wessling (2012)], or different algorithms iteratively solving differential equations like using orthogonal colocalization [Kaldis, Kapantaidakis, Papadopoulos, and Sakellaropoulos (1998)].

Almost any simplifying assumption can be replaced by exactness in exchange for adequate computational resources and time. Yet, in applications that don't need a precise result but rather a good estimation of the outcome methods low in computational demand are preferential. With such a method the dependency of the outcome on various input parameters (like the length and radius of the fibers in a hollow fiber membrane) can be observed on the scale of different orders of magnitude.

In this paper we therefore present a method derived from molecular kinetic theory of gases, statistically generalized to a mesoscopic system, that allows for the prediction of the permeation of a diluted substance present in a feed stream.

This is achieved by using simulation particles that move like individual molecules, but statistically represent an ensemble of molecules whose physical properties (like pressure) the simulation particle carries, and the method was therefore named *Statistical Particle Displacement Model* or **SPDM**. This technique is used to estimate the fraction of particles/molecules that permeate under different boundary conditions and thus allows for a reasonable dimensioning of a hollow fiber module to extract a diluted component from a bulk gas.

2 The Statistical Particle Displacement Model

The SPDM uses diffusion, according to the kinetic gas theory, and convection to model the particle movement within a fiber. Together with the implementation of a membrane permeability, this enables the observation of the concentration distribution within a fiber.

The model was designed to simulate a feed stream flowing through the inside of a hollow fiber membrane with a selective layer on the inside, and a constant pressure on the outside (maintained by e.g. a vacuum pump; see Fig. 1).

The preconditions for this model are, that a laminar flow is required, and that the permeating species is only present in amounts where the permeation of the observed substance does not effect the bulk behavior (therefore constant pressure on the feed side).

These conditions are given when a low pressure drop along the fiber (frictional

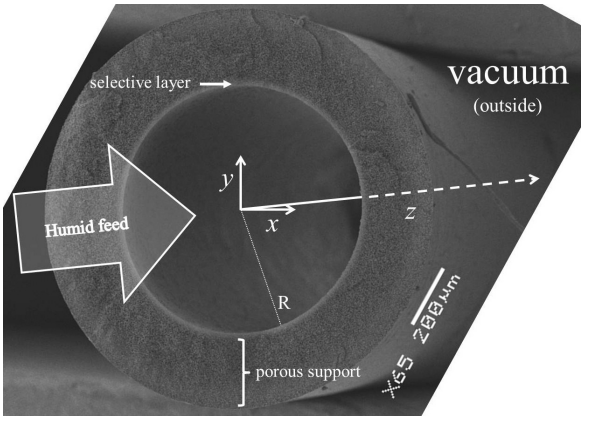

Figure 1: SEM image of a composite hollow fiber membrane of radius R, with the selective coating on the inside of the porous support structure. x, y and z denote the dimensions used in the model.

losses) is desired and the desired substance is only present in diluted form in the feed stream (i.e. water vapor in ambient air). However, this method is also extendable to turbulent flow, assuming a well mixed, homogeneous concentration distribution.

Due to the use of diffusion as transport mechanism towards the membrane, the transport resistance on the feed side can be accounted for completely so that effects like concentration polarization, need not be considered separately.

The membrane implementation as a routine that models the membrane resistance as a rebound probability ensures that a membrane element sees only the local pressure gradient as driving force. Therefore, it takes the depletion of the diluted species along the fiber axis as well as the concentration build-up/depletion in the boundary layer into account.

2.1 Molecular movement within a fiber

The movement of a molecule within a fiber is governed by two main processes: convection and diffusion. For Reynolds numbers that are low enough, the flow through a hollow fiber is laminar($Re \leq 2300$), and turbulence does not occur. Thus the convection in the radial direction ($\vec{r} = (x,y)$, $|r| = \sqrt{x^2+y^2}$) can be neglected. Equally a forced convection along the z-axis (see Fig. 1), by blowing an air stream through the fiber, leads to flow speeds which are orders of magnitude larger than the displacement of a molecule due to diffusion. Therefore the transport mechanisms in a fiber can be separated, and dealt with in two independent manners: convection

along the z-axis and 2-dimensional diffusion in the x-y plane.

Diffusion Below the critical point, when not too close to their phase change, gases behave almost like ideal gases. According to the kinetic gas theory the individual gas molecules are moving, and their displacement can be described by Brownian motion. Their free pathway in a medium determines the diffusion coefficient D. According to Fick's second law interpreted as the probability $\mathscr{P}$, the likelihood of a molecule to be found in $[\vec{x}, +d\vec{x}[$ at a certain point in time t, can be given as

$$\frac{\partial \mathscr{P}(\vec{x},t)}{\partial t} = D\frac{\partial^2 \mathscr{P}(\vec{x},t)}{\partial x^2} \tag{1}$$

with the solution

$$\mathscr{P}(\vec{x},t)d\vec{x} = \frac{1}{(4\pi Dt)^{n/2}} \exp\left(-\frac{\vec{x}^2}{4nDt}\right) d\vec{x} \tag{2}$$

where n is the number of observed dimensions. As previously mentioned the diffusion along the z-axis can be neglected, and the problem can thus be dealt with in a 2-dimensional space. Therefore the position of a molecule after a time t is determined by a Gaussian distribution with a mean value of 0, and a standard deviation of $\sqrt{4Dt}$ which results in a mean squared displacement (MSD) of:

$$MSD = 4Dt \tag{3}$$

Convection To simulate the transport along the z-axis a homogeneous speed distribution is assumed in radial direction (plug flow) with a fixed value $\bar{u}$, assuming that the frictional losses are small enough to not significantly influence this value along the axis.

2.2 The statistical implementation of the kinetic gas theory

By separating the axial transport from the radial transport, the 2- dimensional diffusion problem in the cross-sectional plane can be observed over various simulation steps, determined by the residual time of an air package within the fiber, and Δt, the chosen time interval between two simulation steps.

In order to simulate the movement of water vapor within the fiber, the above mentioned kinetic theory of gases is applied to track the motion of N simulation particles. Although the particles move like individual molecules, they are used to statistically represent all the vapor molecules present in the feed flow according to Eq. 7.

Initially the particles are placed in a uniform random distribution within the circular cross section of the fiber, to represent the well mixed concentration distribution in the feed flow.

The position on the x-axis of each particle after an iteration step, representing the situation Δt seconds later, is determined by

$$x(t_i) = x(t_{i-1}) + \Delta x \tag{4}$$

where Δx is a random number generated according to a normal distribution with a mean of 0, and a standard deviation of

$$\sigma = \sqrt{2D\Delta t} \tag{5}$$

as derived from a 1-dimensional solution for Eq. 2. The same procedure is applied to the y-components of the positions of the particles to determine their new location.

Those particles whose position now lies out of bounds of the fiber cross section ($x^2 + y^2 \geq R$) are considered to have interacted with the membrane. For the idealized example of no permeation resistance, those particles are taken out of the simulation, and the next displacement step is performed on the remaining ones. After $l/\bar{u}\Delta t$ simulation steps the number of particles still within bounds is compared to the initial number of particles, and thus the fraction of simulation particles that permeated can be computed.

2.3 Implementation of the membrane permeability

The gas permeation through a membrane can be described according to [Wijmans and Baker (1995)] as

$$J = P\frac{\Delta p}{\delta_{mem}}\left[\frac{\text{mol}}{\text{m}^2\text{s}}\right] \tag{6}$$

where P is the membrane permeability, Δp is the difference in partial pressure, and δ_{mem} is the thickness of the membrane.

Membrane permeabilities are usually given in the unit of 'Barrer' which is defined at STP (Standard Temperature and Pressure) as $10^{-10}\frac{cm^3(O_2)cm}{cm^2\,s\,cmHg}$ which is equivalent to $3.348\cdot10^{-10}\frac{mol}{s\,Pa\,m^2}$ or simply as $7.5\cdot10^{-18}\frac{m^2}{s\,Pa}$ Some representative values for water vapor permeabilities according to [Metz (2003)] can be seen in Tab. 1.

As mentioned, each simulation particle represents a certain number of molecules (α_i) according to:

$$\alpha_i = \frac{\Delta c_0\,\Delta V}{N}\ [\text{mol}] \tag{7}$$

Table 1: Water vapor permeabilities for different materials

Name	**abbreviation**	**permeability [Barrer]**
Cellulose-Acetate	CA	6 000
Ethyl Cellulose	EC	20 000
Polydimethylsiloxane	PDMS	40 000
Sulfonated Polyetheretherketone	SPEEK	61 000
polyethylene xxide-polybutylene erephthalate	PEO-PBT	104 000

where c_0 is the concentration difference between the inlet feed stream and the permeate side, ΔV is the volume element defined by the displacement along the fiber within a simulation time step ($\Delta z = \bar{u}\ \Delta t$) and the cross sectional area of the fiber, and N is the number of particles used for the simulation. When in a first simulation step according to section 2.2 a number of ν particles move out of bounds, then this number ν represents the initial partial pressure difference between the feed and the permeate side Δp_0. Therefore, a single particle hitting the wall represents the membrane seeing a driving force of

$$\Delta p_i = \frac{\Delta p_0}{\nu}\ [\text{Pa}] \tag{8}$$

According to Eq. 6, this means that from an initial α_i molecules represented by one simulation particle, a number of molecules ($\Delta\alpha_i$) will permeate through the observed membrane area ($\Delta A = 2r\pi\Delta z$) within the time Δt . This number can be written as

$$\Delta\alpha_i = J\Delta t\Delta A = \frac{P}{\delta_{mem}}\frac{\Delta p_0}{\nu}\Delta t\, 2r\pi\Delta z\ [\text{mol}] \tag{9}$$

To account for this number of permeated molecules each particle that moves out of bounds is taken out of the system with a probability $\mathscr{P}$ that is equal to the fraction of molecules theoretically permeating and the number of molecules α_i one simulation particle represents. Using the ideal gas law ($\Delta p = \Delta c\bar{R}T$) this probability can be given as:

$$\mathscr{P} = \frac{\Delta\alpha_i}{\alpha_i} = \frac{\frac{P}{\delta_{mem}}\frac{\Delta p_0}{\nu}\Delta t\, 2r\pi\Delta z}{\frac{\Delta c_0 \Delta V}{N}} = 2\frac{N}{\nu}\frac{P\bar{R}T\,\Delta t}{\delta_{mem}\, r} \tag{10}$$

where $\bar{R}$ is the gas constant, and T the absolute temperature. So if a particle moves out of bounds, a random number is generated (uniform distribution between 0 and

1). If it is smaller or equal to $\mathscr{P}$ then the particle is taken out of the system and considered as permeated. If the random number should be bigger than $\mathscr{P}$ the particle is considered as reflected and thus put back to the initial position before the displacement was added.

A requirement to achieve independence of $\mathscr{P}$ of the particle number N and the time interval Δt is a preceding simulation step. In this step a large number of particles (10^7) is uniformly distributed within an annulus with a width of 4σ of Eq. 2 reaching from the inside to the fiber wall (accounting for 99,9968% of particles that could reach the fiber wall within Δt). The displacement procedure is then performed as described in section 2.2. The number of the extrapolated total number of simulation particles, N_{ext}, and the particles moving out of bounds at such a preceding step, ν_0, are used to calculate a refined ratio N_{ext}/ν_0 that replaces the N/ν term in Eq. 10. This creates a permeation probability for a particle hitting the wall, that is independent of the number of simulation particles used.

The fraction of permeated simulation particles can then be used to calculate the outlet concentration of the feed stream (retentate). As the N particles as a whole represent the concentration difference between inlet and permeate side (Eq. 7), a situation in which all particles have permeated, represents a concentration of the retentate equal to that on the permeate side (the molecules entering the fiber and the ones permeating out are at equilibrium). Thus the retentate concentration at the outlet is given by:

$$c_{ret} = c_{in} - \Delta c \left(1 - \frac{N_{out}}{N_{in}}\right) \tag{11}$$

3 Results and Discussion

In order to evaluate the performance of this SPDM, a model environment for separating water vapor from ambient air was chosen at the following conditions: Air at 30 °C with a water vapor concentration of 0.841 $\mathrm{mol}/\mathrm{m}^3$ (equivalent to 50% relative humidity) is blown through the inside of a composite hollow fiber membrane. The diffusion constant of water vapor in the air is, according to [Massman (1998)]: $D = 0.2178 \cdot 10^{-4} \left(\frac{T}{T_0}\right)^{1.81}$, with T and T_0 being the working temperature in K, and the reference temperature of 273.15 K respectively. The permeate pressure is kept at a constant pressure of 10 mbar which is the vapor pressure equivalent to a concentration of 0.403 $\mathrm{mol}/\mathrm{m}^3$. Due to a very porous structure of the hollow fiber, its transport resistance is neglected, leaving the selective layer with a thickness of 3 μm as sole resistance contributor.

3.1 Parameter independence of outcome

The simulation relies on 2 parameters that can be chosen freely, and whose magnitude directly effects the computational time, as well as the precision of the outcome: the number of particles N used to represent the water molecules as a whole and governing the statistics of the simulation, and the time interval Δt between two simulation steps that influence the mean step size according to Eq. 3.

Both parameters need to be chosen in a range in which the fluctuation or deviation of the result, is negligible as compared to the desired precision of the outcome. For that purpose a 5 cm long fiber was modeled 4 times, with a diameter of 1.4 mm and a mean flow speed of 6.57 $^{m}/_{s}$, varying the time difference between two simulation steps Δt (while keeping the particle number constant at $N = 10^6$) and varying the number of simulation particles N (with constant $\Delta t = 10^{-6}$).

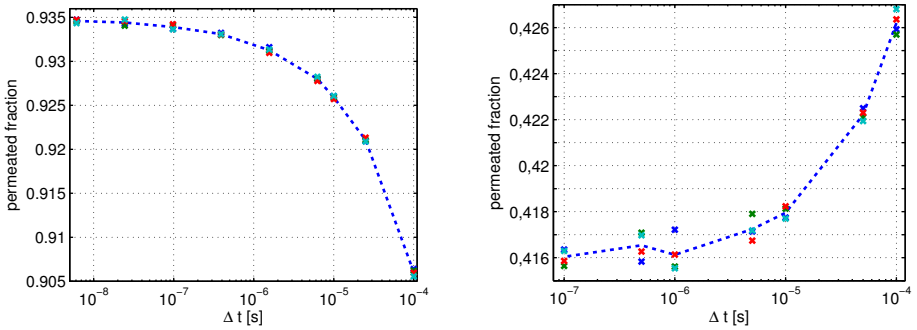

(a) without membrane resistance (b) with membrane resistance

Figure 2: Time step dependence of the fraction of permeated particles without (a) and with (b) membrane resistance. The dotted line connects the mean values of the 4 simulations for each x-value. l=0.05 m, r=7e-4 m, $\bar{u}$=6.57 m/s, N=1e6, P=104000 Barrer (b-only)

The results show (compare Fig. 2) that in the case without membrane resistance, a time step of $\Delta t = 10^{-5}$ s leads to results that lie within 1% of the final value (a) ($|\mu_{\Delta t=1e-5s} - \mu_{\Delta t=6.1e-9s}| = 0.87\%$,$\sigma_{\Delta t=1e-5s} = 0.21\%$.) and in the case of the membrane with transport resistance around 0.5% of the final value (b) ($|\mu_{\Delta t=1e-5s} - \mu_{\Delta t=1e-7s}| = 0.19\%$,$\sigma_{\Delta t=1e-5s} = 0.02\%$). Yet, the computational time is relatively low ($t_{mean} = 105.4$ s for simulation with membrane resistance, $N = 1e6$, with 1 Core of 2,5 GHz, Intel® T9300 - compare Fig. 3). Therefore, this value was chosen for further simulations.

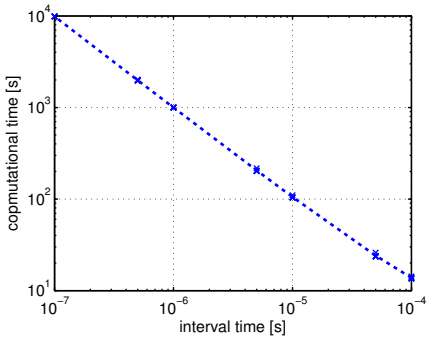

Figure 3: Time step dependence of total simulation time. The dotted line connects the mean values for each x-value. l=0.05 m, r=7e-4 m, $\bar{u}$=6.57 m/s, N=1e6, 1 CPU at 2.5 GHz

In a similar way the stability of the result with varying particle number N was shown, with the above settings and a time step of Δt=1e-6 s (Fig. 4: $|\mu_{N=1e5} - \mu_{N=5e6}| < 0.007\%$,$\sigma_{N=1e5} = 0.21\%$.)

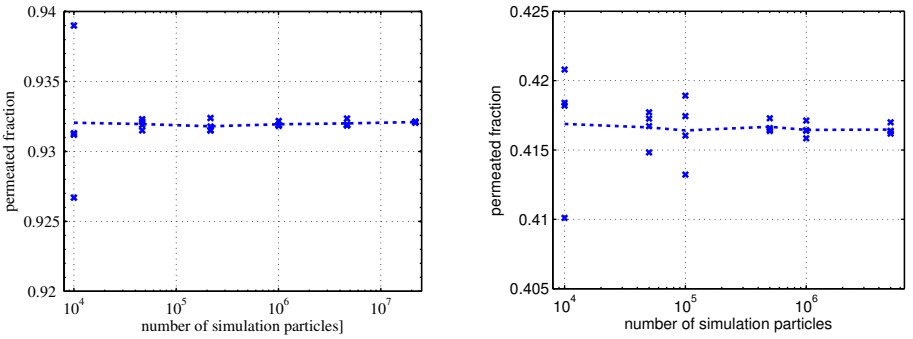

(a) ideal membrane (b) real membrane

Figure 4: Simulation particle dependence of the fraction of permeated particles. l=0.05 m, r=7e-4 m,$\bar{u}$=6.57 m/s, Δt=1e-6, P=104000 Barrer (b-only)

With the determination of these values, the physical parameters (length, radius, feed speed) can now be varied to get the fraction of permeated particles. The values chosen for were $N = 10^5$ and $\Delta t = 10^{-5}$.

3.2 Validation using CFD simulation

In order to estimate the relative error of the plug flow simplification, various situations were modeled with above mentioned SPDM approach, as well as with a commercial multi-physics CFD (Computational Fluid Dynamics) software (Comsol). The mesh is chosen in such a way (5000 elements), that a much refined mesh (20000 elements) does not lead to any noticeable change of the permeated fraction (pf) on the scale of the model comparisons ($max\left(|pf_{mesh5000} - pf_{mesh20000}|\right) < 0.66\%$). The model is then solved for the velocity field first, to use these vectors as basis for the transport of diluted species.

3.2.1 The ideal membrane: no transport resistance

To investigate the effect of the flow profile, the 2 methods were first compared in a model without membrane resistance. In the CFD simulations, the inlet concentration and the fiber wall concentration are thus set at constant concentration and the outlet flux is compared to the inlet to evaluate the fraction of permeated molecules. These data can then be compared to the results of the SPDM, and it shows that for a fixed radius the maximum difference is reached when the length of the fiber is equal to the hydrodynamic entrance length, l_e, as can be seen in Fig. 5. l_e is defined as the distance that is required until the flow profile in a pipe reaches its final parabolic form, and can be calculated, according to [Wang (1982)], via: $l_e = 0.02866 \cdot Re \cdot d$, with Re being the Reynolds number and d the diameter in m.

Simulations with a different radius (r=0.4 mm) and different feed speeds have confirmed this assumption, and generally shown, that for a fixed radius and the plug flow simplification, the permeation fraction as a function of entrance length, is independent of the flow speed (as long as $Re \leq 2300$). This is of course due to the fact that for a certain radius, the time required for an air parcel to reach the entrance length is the same for all speeds as $l_e/\bar{u} = const \cdot d$, where $const$ is a constant that is determined by the air properties.

The peak at $l = l_e$ (vertical line) can be understood, as the developing flow profile $l < l_e$ resembles the plug flow more and therefore the simplification of the statistical particle displacement resembles these circumstances better. At $l = l_e$ the flow profile is fully developed, and the concentration within the fiber still relatively high, which means that a faster flux in the center of the fiber transports more molecules out of the system. At $l > l_e$ the total concentration is already reduced and thus the effect of the parabolic flow profile less pronounced than at $l = l_e$.

Although the deviation can lead to an estimation error of about 14% (simulation with r=0.4 mm) of the total permeation (the error gets smaller for bigger radii (as was seen in Fig. 5) due to the less steep flow profile within the fiber),this method

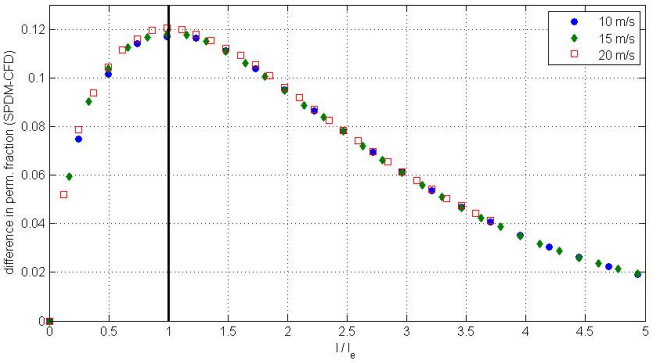

Figure 5: Difference between the permeated fraction of the SPDM and the CFD model, as function of the entrance length for different feed speeds. r=0.75 mm

still proofs worthwhile for getting an estimation of a fiber module and the dimensioning which would be most desirable.

3.2.2 The realistic membrane: permeability as material property

If the membrane permeability is also taken into account, all the physical properties (length, radius, feed speed, membrane permeability, pressure drop across the membrane) can be considered, and the amount of gas permeating through different fibers can be simulated (see Fig. 6. It can be seen that an increasing permeability reduces the concentration along the fiber, and that the use of long fibers with high permeability can lead to inefficient use of the membrane area.

In the CFD simulations a concentration dependent outflow flux through a membrane element can be prescribed. The coupling of this outflow to the membrane permeability and the flux according to Eq. 6 can be achieved via

$$\Delta p = \frac{n_{local} * \bar{R} * T}{V} - \frac{n_{perm} * R * T}{V} = (c_{local} - c_{perm}) * \bar{R} * T \tag{12}$$

The comparison (see Fig. 7(a)) between the two models shows a level of agreement much higher than in the case of the infinitely permeable membrane (Fig. 5). This can be easily understood as a higher permeation resistance means a higher concentration at the outer layers and thus a more equal concentration distribution in the cross section of the fiber. As mentioned previously about the plug flow and parabolic flow profile, this means, that the overestimation of permeated particles will get less. Besides, at some point (at very low permeability) the transport of

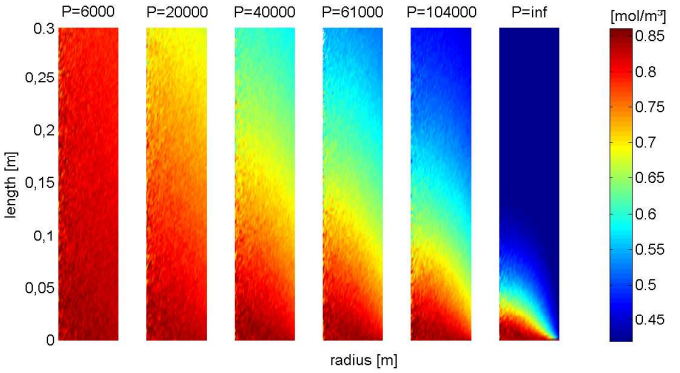

Figure 6: The concentration distribution in a hollow fiber coated with membranes of different permeabilities (P in Barrer). The color bar indicates the concentration in $[\mathrm{mol/m^3}]$, and the permeabilities correspond to the water vapor permeability for (from left to right): CA, EC, PDMS, SPEEK, PEO-PBT and an ideal membrane, according to Tab. 1 ; l=0.05 m, r=0.75 mm, $\bar{u}$=10 m/s, $c_{feed} = 0.403$ mol/m^3, $c_{perm} = 0.841$ mol/m^3

particles at the boundary layer for which a no slip condition would apply, will influence the outcome more than the higher flux at the center of the fiber. This leads to an underestimation of the plug flow SPDM simulation as compared to the CFD simulation (as it is the case for P=6000 Barrer in Fig. 7(b))

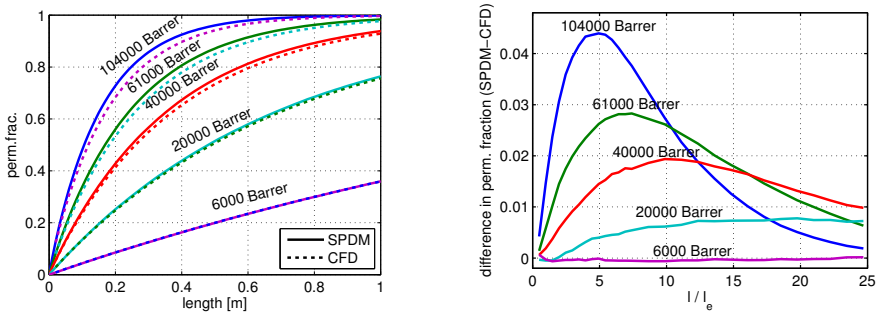

(a) CFD and SPDM (b) with membrane

Figure 7: Predicted permeation fractions for CFD simulations and the SPDM (a) and their difference (b) for different permeabilities. r=0.75 mm, $\bar{u}$=10 m/s, l was varied from 2 to 100 cm

Using this method the desired identification of an ideal operational window, as mentioned in the introduction, can be determined. In terms of minimizing the energy demand for driving the feed flow, Hagen-Poiseuille law [Bird, Stewart, and Lightfoot (1960)] together with corrections for the entrance effects according to [Wang (1982)] can be used to estimate the pressure drop along a fiber and thus the required work to push an air parcel through these fibers. Normalizing these numbers with the simulated vapor permeation gives a relative energy requirement per mole of water vapor, simulated for different feed speeds (see Fig. 8). Especially for higher speeds and small lengths (see Fig 8(b) the increased energy requirement due to the entrance effects can be seen. Also the trend that the energy requirement for driving a feed flow that results in the permeation of 1 mol of water vapor is proportional to the fiber length and the feed speed, and indirectly proportional to the radius can be seen. This is of course due to the fact that in these scenarios the retentate stream is still high in vapor concentration, and thus the driving force for the permeation stays high along the whole fiber. Yet to determine the ideal operational window for such a process completely, the effective use of the membrane area as well as the module have to be considered too.

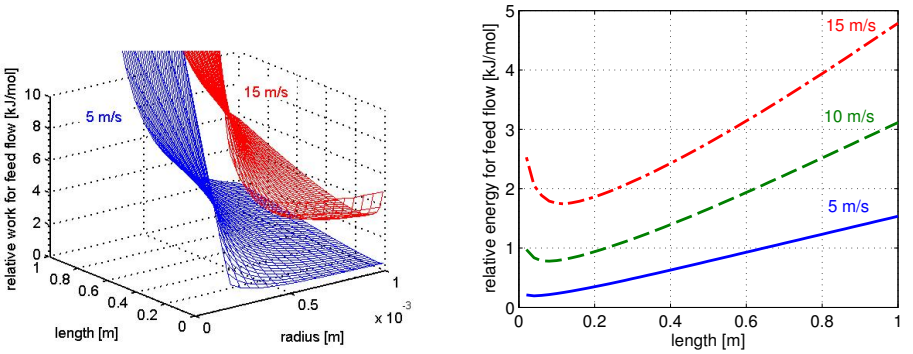

(a) scan over various parameters

(b) specific results for r=0.75 mm

Figure 8: Energy needed to drive the feed flow required to get a permeation of 1 mol of water vapor for different lengths, radii and feed speeds (5, 10 and 15 m/s - bottom to top). The membrane permeability is 104000 Barrer.

4 Conclusion

In conclusion, it has been shown, that the SPDM is a valid tool to estimate the fraction of molecules permeating through a hollow fiber membrane. Even though it is not the most exact model in its prediction accuracy, and has its limitations in

laminar applications and low concentrations of the desired permeating substance, its advantages lie in its easy implementation, the (computational) cost effectiveness and with its simplicity also the requirement of relatively little RAM memory. The ability to adapt all physical parameters, and the possibility to extrapolate results from a certain length and feed speed to other values via the hydrodynamic entrance length, allows for a fast scan over a wide range of parameters.

Thus, the right dimensioning of hollow fiber membrane module (parallel arrangement of multiple fibers), can be found to determine an operational window, in which the minimum work for driving the feed flow can be determined for a given set of parameters. This is a useful application when a high energy and cost efficiency is required as is the case for the production of drinking water [Bergmair, Metz, de Lange, and van Steenhoven (2012)].

Acknowledgement: This work was performed in the TTIW-cooperation framework of Wetsus, centre of excellence for sustainable water technology (www.wetsus.nl). Wetsus is funded by the Dutch Ministry of Economic Affairs, the European Union Regional Development Fund, the Province of Fryslân, the City of Leeuwarden and the EZ/Kompas program of the "Samenwerkingsverband Noord-Nederland". The authors like to thank the participants of the research theme, in particular P.M. Biesheuvel, for the fruitful discussions and their financial support.

References

Baker, R. (2002): Future directions of membrane gas separation technology. *Industrial & Engineering Chemistry Research*, vol. 41, no. 6, pp. 1393–1411.

Bergmair, D.; Metz, S. J.; de Lange, H. C.; van Steenhoven, A. A. (2012): Modeling of a water vapor selective membrane unit to increase the energy efficiency of humidity harvesting. *Journal of Physics: Conference Series*, vol. 395, no. 1, pp. 012161.

Bird, R.; Stewart, W.; Lightfoot, E. (1960): *Transport Phenomena*. John Wiley & Sons.

Cruz, P.; Santos, J.; Magalhaes, F.; Mendes, A. (2005): Simulation of separation processes using finite volume method. *Computers & chemical engineering*, vol. 30, no. 1, pp. 83–98.

Fritzmann, C.; Löwenberg, J.; Wintgens, T.; Melin, T. (2007): State-of-the-art of reverse osmosis desalination. *Desalination*, vol. 216, no. 1, pp. 1–76.

Ghidossi, R.; Veyret, D.; Moulin, P. (2006): Computational fluid dynamics applied to membranes: State of the art and opportunities. *Chemical Engineering and Processing: Process Intensification*, vol. 45, no. 6, pp. 437–454.

Kaldis, S.; Kapantaidakis, G.; Papadopoulos, T.; Sakellaropoulos, G. (1998): Simulation of binary gas separation in hollow fiber asymmetric membranes by orthogonal collocation. *Journal of membrane science*, vol. 142, no. 1, pp. 43–59.

Marriott, J.; Sørensen, E. (2003): A general approach to modelling membrane modules. *Chemical engineering science*, vol. 58, no. 22, pp. 4975–4990.

Marriott, J.; Sørensen, E.; Bogle, I. (2001): Detailed mathematical modelling of membrane modules. *Computers & Chemical Engineering*, vol. 25, no. 4-6, pp. 693–700.

Massman, W. J. (1998): A review of the molecular diffusivities of h2o, co2, ch4, co, o3, so2, nh3, n2o, no, and no2 in air, o2 and n2 near stp. *Atmospheric Environment*, vol. 32, no. 6, pp. 1111–1127.

Metz, S. (2003): *Water vapor and gas transport through polymeric membranes*. PhD thesis, University of Twente, 2003.

Scholz, M.; Harlacher, T.; Melin, T.; Wessling, M. (2012): Modeling gas permeation by linking nonideal effects. *Industrial & Engineering Chemistry Research*.

Shannon, M.; Bohn, P.; Elimelech, M.; Georgiadis, J.; Mariñas, B.; Mayes, A. (2008): Science and technology for water purification in the coming decades. *Nature*, vol. 452, no. 7185, pp. 301–310.

Smitha, B.; Suhanya, D.; Sridhar, S.; Ramakrishna, M. (2004): Separation of organic-organic mixtures by pervaporation - a review. *Journal of Membrane Science*, vol. 241, no. 1, pp. 1–21.

Wang, Z.-Q. (1982): Study on correction coefficients of liminar and turbulent entrance region effect in round pipe. *Applied Mathematics and Mechanics*, vol. 3, no. 3, pp. 433–446.

Wijmans, J. G.; Baker, R. W. (1995): The solution-diffusion model: a review. *Journal of Membrane Science*, vol. 107, no. 1-2, pp. 1–21.